

# Sintering behaviour of CuO-doped SnO<sub>2</sub>

Jérôme Lalande, Rolande Ollitrault-Fichet, Philippe Boch \*

*Ecole Supérieure de Physique et de Chimie Industrielles, 75005 Paris, France*

Received 1 February 2000; received in revised form 27 April 2000; accepted 11 May 2000

## Abstract

The sintering behaviour of CuO-doped SnO<sub>2</sub> ceramics was studied. Additive-free SnO<sub>2</sub> materials do not densify after heat treatment to 1400°C, whereas materials doped with 0.5–0.75 wt.% CuO densify to 98% of theoretical. Copper oxides (CuO/Cu<sub>2</sub>O) experience reduction and re-oxidation phenomena. There is no evidence of high vaporisation of SnO<sub>2</sub>, nor of liquid formation at low temperature (< 1000°C) in the CuO–SnO<sub>2</sub> system. This suggests that CuO acts by grain-boundary mechanisms. © 2000 Published by Elsevier Science Ltd. All rights reserved.

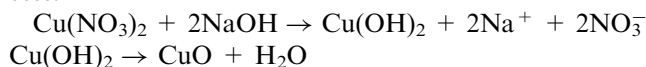
*Keywords:* CuO; Microstructure-final; Sintering; SnO<sub>2</sub>

## 1. Introduction

Tin dioxide (SnO<sub>2</sub>) is a semiconductor (n-type) with wide band gap, which exhibits interesting properties for many applications, such as gas sensors, electrodes for glass melting furnaces, electrochromic devices, crystal displays, photodetectors, solar cells, protective coatings, and various electrical devices. Unfortunately, additive-free SnO<sub>2</sub> exhibits poor sinterability, seemingly because of the dominance of non-densifying mechanisms for mass transport, such as surface diffusion and evaporation–condensation,<sup>1–3</sup> which only promote pore coarsening and grain growth. Even though the use of very fine SnO<sub>2</sub> powders compacted under very high pressure<sup>4</sup> or the use of hot isostatic pressing<sup>5</sup> offer solutions for preparing highly-densified SnO<sub>2</sub> ceramics, the best strategy is to employ sintering additives. Various oxides have been studied as sintering aids to densify SnO<sub>2</sub>, for example ZnO,<sup>3</sup> Sb<sub>2</sub>O<sub>3</sub>,<sup>6</sup> V<sub>2</sub>O<sub>5</sub>,<sup>7</sup> Nb<sub>2</sub>O<sub>5</sub>,<sup>8</sup> CoO and MnO,<sup>2,9</sup> Li<sub>2</sub>O,<sup>10</sup> or CuO.<sup>11–13</sup> CuO is particularly effective, because low concentrations (≈ 1 mol%) of CuO are enough to yield nearly-full densification of SnO<sub>2</sub>-based ceramics. The role of CuO was twice. At high temperatures, it was considered to promote liquid phase sintering,<sup>11</sup> whereas at low temperatures it was considered to act through surface diffusion mechanisms.<sup>12</sup> The present work brings complementary results on the sintering behaviour of CuO-doped SnO<sub>2</sub> ceramics.

## 2. Experimental procedure

Mechanical mixing rarely ensures mixture homogeneity, in particular when one has to add a minute amount of additives to a major constituent. It is the reason why we used a precursor-plus-powder route, where the SnO<sub>2</sub> powders were impregnated with a CuO-containing aqueous solution. The SnO<sub>2</sub> powders (Goldschmidt) were 99.98% pure, with BET surface area of ≈ 3.7 m<sup>2</sup> g<sup>-1</sup> and mean grain size of ≈ 0.7 μm. The CuO precursor was 99.5% pure Cu(NO<sub>3</sub>)<sub>2</sub>·3H<sub>2</sub>O (Strem Chemicals). The formation of CuO is a two-stage process:<sup>14</sup>



Cu(II) hydroxide precipitates by addition of sodium hydroxide, then unstable Cu(OH)<sub>2</sub> dehydrates toward insoluble CuO.

The SnO<sub>2</sub>-based materials were doped with various quantities of CuO: 0.25, 0.5, 0.75, 1.0, 1.25, 1.5, 2.25, 3.0, and 7.5 wt.%. Suitable quantities of SnO<sub>2</sub> and Cu(NO<sub>3</sub>)<sub>2</sub>·3H<sub>2</sub>O were mixed in a beaker with a minimum amount of water (approximately 200 ml for 20 g of powders). After dissolution of copper nitrate, the sodium hydroxide was added. After precipitation of CuO, there was a succession of stirring and washing stages with demineralised water to eliminate the soluble nitrate and sodium ions. An organic binder (polyethylene glycol, PEG) was added to the CuO-doped SnO<sub>2</sub> powders and the mixture was ultrasonically mixed, then dried at 110°C and deagglomerated. Pellets

\* Corresponding author. Fax: +33-14079-4750.  
E-mail address: philippe.boch@espci.fr (P. Boch).

(13 mm in diameter and 1.8 mm in thickness) were compacted by uniaxial pressing under a pressure of 200 MPa. The green density of pressed pellets was  $\approx 65\%$  of theoretical. The PEG pyrolysis and subsequent sintering treatments were carried out in normal atmosphere.

Complementary experiments were carried out on materials with high CuO contents (20, 40, 50, 60, 70, and 80 wt.%), prepared by direct mixing of SnO<sub>2</sub> and CuO powders.

Characterisation tests were done using X-ray diffraction (XRD), DTA-TG experiments, dilatometry, and scanning electron microscopy (SEM) equipped with X-ray microanalysis.

### 3. Results and discussion

#### 3.1. XRD

The phase diagram CuO–SnO<sub>2</sub> is imperfectly known, but there is no record of any mixed copper/tin oxide. Dolet et al.<sup>11</sup> have so far found limited solubility of CuO in the SnO<sub>2</sub> lattice yet. The radii of Sn<sup>4+</sup> and Cu<sup>2+</sup> are quite close (0.069 and 0.073 nm, respectively, according to Shannon and Prewitt tables), which means a small solubility of CuO in SnO<sub>2</sub> is not expected to change the cell parameters of the solid solution very much. In fact, the sensitivity of XRD is insufficient to allow the detection of a low concentration of any Cu-rich secondary phase or of a solid-solution with lattice parameters very close to those of SnO<sub>2</sub>. In materials with low CuO contents, therefore, XRD cannot be used to discriminate between the two possible cases of (i) copper segregated in Cu-containing secondary phases or (ii) copper dissolved in a SnO<sub>2</sub>-based solid solution. We found  $a=0.4738$  nm and  $c=0.3187$  nm for the starting powders and the heat-treated powders as well, to be compared with JCPDS data of  $a=0.47382$  nm and  $c=0.31871$  nm (JCPDS, card No. 41-1445). The cell (tetragonal, rutile-type structure) contains two tin atoms and four oxygen atoms, which leads to theoretical density of  $6.99$  g cm<sup>-3</sup>, very close to the value of  $6.97 \pm 0.08$  g cm<sup>-3</sup> we measured by pycnometry.

In high-CuO ([CuO] > 7.5%) materials, however, the precipitation of CuO is large enough to allow Bragg's peaks of CuO to be visible besides those of SnO<sub>2</sub>.

#### 3.2. Dilatometry

Fig. 1 shows dimension changes ( $\Delta L/L$ ) versus temperature and Fig. 2 shows the corresponding shrinkage rate ( $d[\Delta L/L]/dt$ ), for dilatometry experiments carried out using a heating rate of  $5^\circ\text{C min}^{-1}$  from room temperature to the maximum temperature of  $1400^\circ\text{C}$ , then a cooling rate of  $10^\circ\text{C min}^{-1}$ . Table 1 gives the relative density versus CuO content of materials sintered

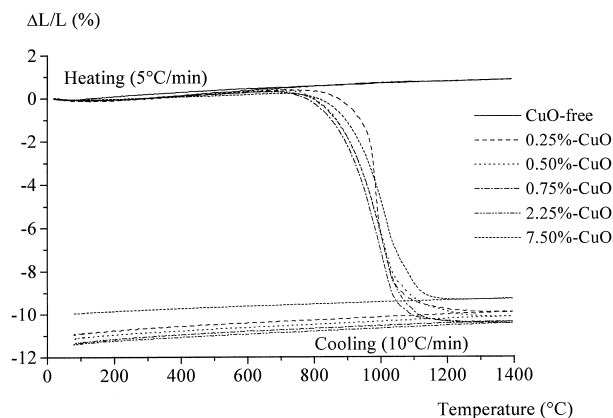


Fig. 1. Dilatometry results for CuO-doped SnO<sub>2</sub> ceramics.

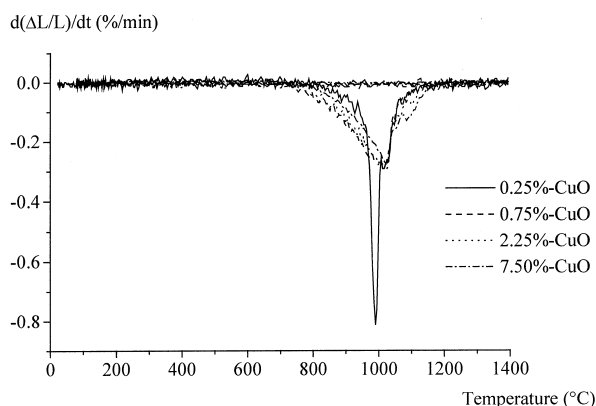


Fig. 2. Shrinkage rate vs. temperature for CuO-doped SnO<sub>2</sub> ceramics (heating and cooling rates as in Fig. 1).

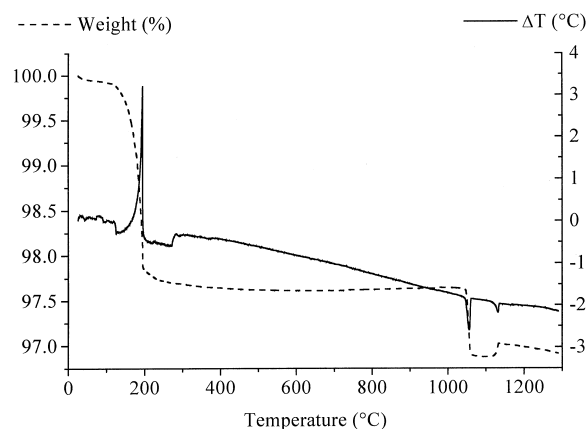


Fig. 3. DTA–TG curves for a 7.5%-CuO SnO<sub>2</sub> material. Heating rate:  $5^\circ\text{C min}^{-1}$  from 20 to  $125^\circ\text{C}$ ,  $1^\circ\text{C min}^{-1}$  from 125 to  $275^\circ\text{C}$ , and  $5^\circ\text{C min}^{-1}$  from 275 to  $1300^\circ\text{C}$ .

to  $1400^\circ\text{C}$  using the same heating and cooling rates than those used for the dilatometry experiments.

As expected, CuO-free SnO<sub>2</sub> does not exhibit any significant densification, even after sintering at the highest temperature we explored ( $1400^\circ\text{C}$ ). Adding small

Table 1  
Relative densities ( $\rho/\rho_0$ ) of CuO-doped SnO<sub>2</sub> ceramics heated to 1400°C<sup>a</sup>

CuO content (wt.%)	0.0	0.25	0.5	0.75	1.0	1.25	1.5	2.25	3.0	7.5
$\rho/\rho_0$ (%) (after treatment at 1400°C)	70	96	98	98	97	97	97	96	96	94

<sup>a</sup> Heating and cooling rates as in Fig. 1.

amounts of CuO dramatically increases densification ( $\rho/\rho_0$ ) and, therefore, the CuO-doped materials can be sintered to high densities. The material with 0.25 wt.% CuO reaches 96.5% of theoretical whereas the materials with 0.5 or 0.75 wt.% culminate to 98%. High CuO concentrations are less favourable yet.

Whatever the CuO contents, the shrinkage rate exhibits a well-marked peak at about 1000°C (995°C for 0.25 wt.% CuO and 1020–1030°C for higher concentrations in CuO). In CuO-rich materials, there is a supplementary weak peak at about 1100°C.

### 3.3. DTA–TG

DTA–TG experiments (not represented here) conducted on CuO-free SnO<sub>2</sub> show that there is no weight loss below  $\approx 1300^\circ\text{C}$  and that the weight loss at 1400°C is still at a low level of  $\approx 0.15\%$ . These data contradict the allegation of a vaporisation of SnO<sub>2</sub> to give SnO at  $\approx 1100^\circ\text{C}$  and, therefore, do not support the assumption that vaporisation is the main cause of low densification.

Fig. 3 shows the DTA–TG curve for a 7.5%-CuO SnO<sub>2</sub> material. The exothermic DTA peak and the weight loss just below 200°C are due to the pyrolysis of the PEG binder. The events at  $1050 \pm 10^\circ\text{C}$  (endothermic peak associated with weight loss) and at  $1130 \pm 10^\circ\text{C}$  (endothermic peak associated with weight gain) are sensibly proportional to the CuO content. DTA–TG experiments (not represented here) conducted on plain CuO materials show similar effects, which demonstrates that the peaks are related to CuO only, not to SnO<sub>2</sub>.

The binary diagram Cu<sub>2</sub>O–CuO<sup>15–17</sup> indicates that CuO reduces to Cu<sub>2</sub>O at temperatures slightly superior to 1000°C. Cu<sub>2</sub>O melts at  $\approx 1230^\circ\text{C}$ . There is a eutectic between Cu<sub>2</sub>O and CuO with melting temperature at  $\approx 1075^\circ\text{C}$  for  $p\text{O}_2 = 0.47$  atm and  $\approx 1090^\circ\text{C}$  for  $p\text{O}_2 = 1$  atm.<sup>11</sup>

If the reduction reaction from CuO to Cu<sub>2</sub>O is complete, one obtains:

$$m(\text{Cu}_2\text{O}) = m(\text{CuO}) \times M(\text{Cu}_2\text{O})/2M(\text{CuO})$$

where  $M$  is molar weight.

This means the weight change of the whole sample is:

$$\Delta m/m = [m(\text{Cu}_2\text{O}) - m(\text{CuO})]/[m(\text{SnO}_2) + m(\text{CuO})]$$

$$\Delta m/m = -0.1(y\% \text{CuO})$$

where  $y\%$  CuO is the percentage of CuO.

For the first endothermic peak at  $\approx 1050^\circ\text{C}$ , the DTA results for 3 and 7.5% CuO materials are:

$$\begin{aligned} \Delta m/m &= -0.30\% & \text{when } y\% \text{ CuO} &= 3\% & \text{and} \\ \Delta m/m &= -0.73\% & \text{when } y\% \text{ CuO} &= 7.5\% \end{aligned}$$

The close agreement between the calculated and experimental data indicates that the events at  $T \approx 1050^\circ\text{C}$  (i.e. the TG weight loss and the DTA endothermic peak) must be due to the reduction of CuO to Cu<sub>2</sub>O. This agreement also confirms that the synthesis route we used was effective to yield the copper concentrations that were chosen.

The events at  $T \approx 1130^\circ\text{C}$ , i.e. the small DTA endothermic peak and the associated TG weight gain, lead to

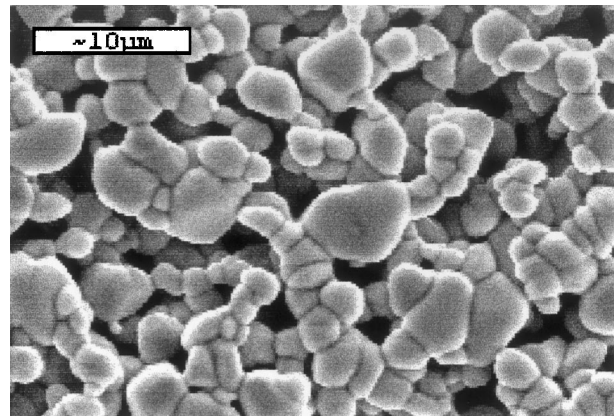


Fig. 4. CuO-free ceramics sintered 2 h at 1400°C.

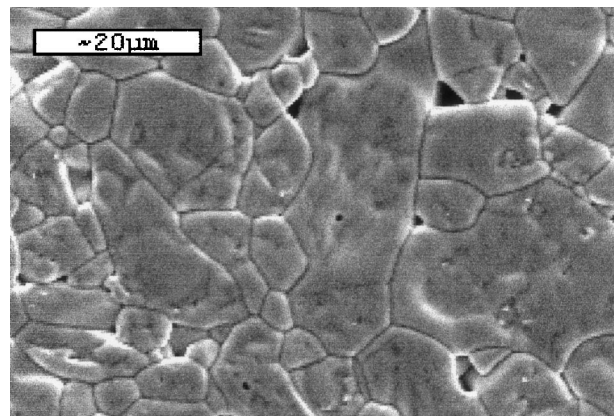


Fig. 5. 0.75%-CuO ceramics sintered 2 h at 1400°C.

suspect the role of a liquid phase<sup>11</sup> and of sorption phenomena, which can yield partial re-oxidation of  $\text{Cu}_2\text{O}$ . To check this, we carried out XRD data on samples quenched from 1000, 1090, or 1140°C to room temperature, using materials with high CuO contents (20, 40, 50, 60, 70, and 80%). The results are that the samples quenched from 1000°C contain CuO, those quenched from 1090°C contain  $\text{Cu}_2\text{O}$ , and those quenched from 1140°C contain a mixture of CuO and  $\text{Cu}_2\text{O}$ . This confirms that the first event (at  $\approx 1050^\circ\text{C}$ ) is a reduction of CuO to  $\text{Cu}_2\text{O}$  whereas the second event (at  $\approx 1130^\circ\text{C}$ ) is a partial re-oxidation of  $\text{Cu}_2\text{O}$  to CuO. The re-oxidation is partial only, which implies that the weight gain is smaller than the weight loss associated with the reduction. In the same temperature range, there is partial melting of copper oxides.

Fig. 3 corresponds to on-heating DTA–TG experiments. On-cooling DTA–TG experiments (not represented here) show one event only, a weight gain at  $\approx 1045^\circ\text{C}$ . This indicates that there is an hysteresis, with delay in solidification and re-oxidation phenomena. The re-oxidation of  $\text{Cu}_2\text{O}$  to CuO is not complete, as shown

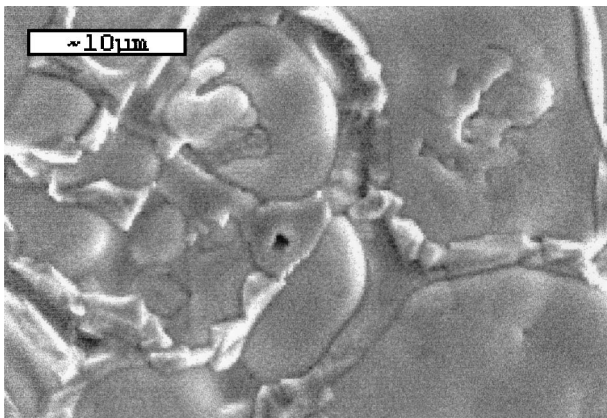


Fig. 6. 7.5%-CuO ceramics sintered 2 h at 1275°C.

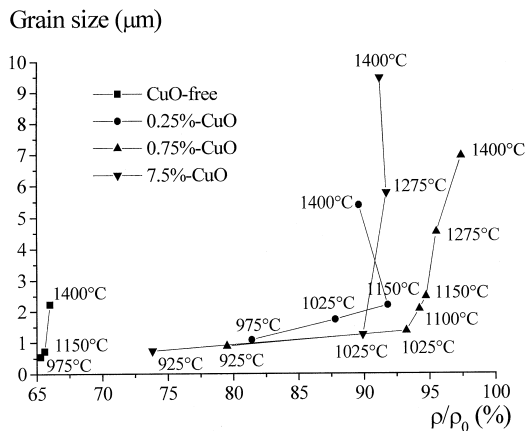


Fig. 7. Grain size vs. densification for CuO-free and CuO-containing ceramics, sintered for 2 h at temperatures as indicated.

by XRD experiments which indicate the presence of  $\text{Cu}_2\text{O}$  residues in samples cooled to room temperature.

### 3.4. SEM

SEM observations were conducted on ceramics sintered for 2 h at temperatures ranging from 925 to 1400°C. The samples were diamond polished (grits from 20 to 1 μm) and thermally etched for 1 h at 50 to 100°C below the sintering temperature. Figs. 4–6 show some examples of SEM photomicrographs. CuO-free  $\text{SnO}_2$  ceramics sintered at 1400°C (Fig. 4) are not densified but they have experienced noticeable grain growth, with final grains much larger than initial powder particles. This confirms that only non-densifying mechanisms operate, presumably surface diffusion because vaporisation does not seem to be marked. In contrast, the CuO-containing ceramics are well densified. The  $\text{SnO}_2$  grains are surrounded by an intergranular phase which forms a thin layer in the low-CuO (e.g. 0.75 wt.%) materials (Fig. 5) and a thick layer in the high-CuO (e.g. 7.5 wt.%) materials (Fig. 6). X-ray microanalyses (not presented here) show that this intergranular phase is copper rich, which means it corresponds to copper-oxide residues. The on-cooling DTA experiments show that the Cu-containing liquid phase solidifies to  $\text{Cu}_2\text{O}$ , which oxidises to CuO at temperatures below  $1035 \pm 10^\circ\text{C}$ . This oxidation<sup>18</sup> results in a volume increase of  $\approx 5\%$ , which is expected to cause dilatometric stress. All SEM observations confirm, therefore, that the solubility of copper in tin oxide is low. We observed, however, that long-duration (15 h) treatments allow limited solubility of CuO within  $\text{SnO}_2$  and, therefore, reduce the quantity of intergranular, Cu-rich precipitates. These results are in good agreement with those of Dolet et al.<sup>12</sup>

Quantitative image analysis was conducted using Scion Image<sup>19</sup> software. Ten SEM images taken at random location on the polished surface of each specimen were captured as  $256 \times 176$  digital-image computer files. The magnification was chosen so as to display 30–40 grains in every image, a number that allows acceptable sampling confidence. After the grain-boundary contrast had been reinforced by using a paint-tool software, images were segmented by applying a grey-level threshold to create binary images. The procedures of grain counting and area estimates were then carried out. The particles, observed on a two-dimensional plane, were randomly cut during polishing, so that their apparent size was lower than the actual one. Assuming a spheroidal shape, the 2D diameter has to be multiplied by  $\approx 1.27$  to give the 3D diameter.

Based on image analysis data, Fig. 7 shows the trajectory of grain size versus densification.<sup>22</sup> One can distinguish (i) a first stage of fast densification rate with no grain growth, until more than 90% of theoretical density, and (ii) a second stage of low densification rate but fast

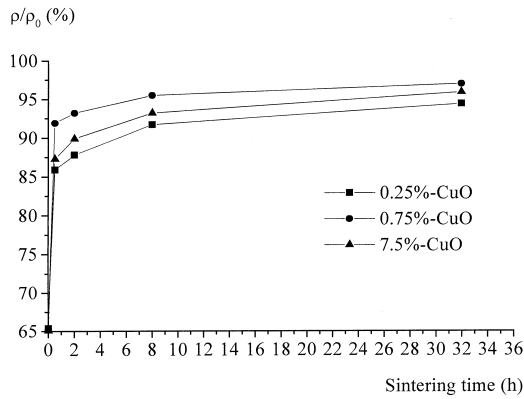


Fig. 8. Densification vs. sintering time for CuO-doped ceramics sintered at 1025°C.

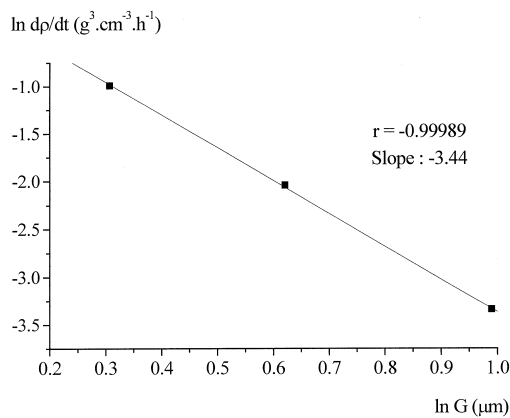


Fig. 9.  $\ln(d\rho/dt)$  vs.  $\ln(G)$  for a 0.75%-CuO ceramic sintered at 1025°C.

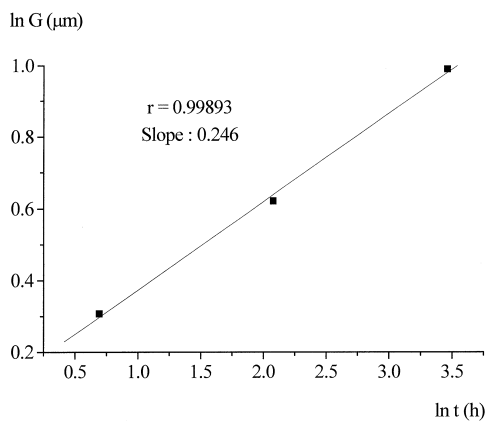


Fig. 10.  $\ln$  (grain size) vs. soaking time for a 0.75%-CuO ceramic sintered at 1025°C.

grain growth. The very fast grain growth experienced by the 7.5%-CuO material leads to pore entrapment in intragranular location, which hinders full densification. The critical point<sup>22</sup> is at about 92% density and 1.5 μm grain size. The best results were found for the 0.75%-CuO material, which exhibits slower grain growth and can, therefore, reach higher densification.

Fig. 8 shows the influence of soaking time on densification for materials sintered at 1025°C. Densification develops very fast at early times, then tends toward a plateau. The respective roles of time and temperature in 0.75%-CuO materials were illustrated by noting that similar densities were obtained after 2 h at 1400°C (Fig. 7) or 32 h at 1025°C (Fig. 8).

The densification and grain growth kinetics were studied in the 0.75%-CuO material sintered at 1025°C. Figs. 9 and 10 show the graphs of  $\ln(d\rho/dt)$  vs.  $\ln(G)$  and  $\ln(G)$  vs.  $t$ , respectively,  $\rho$  being relative density,  $G$  average grain size, and  $t$  time. For densification, the slope has a value of  $-3.44$  (regression coefficient of 0.99989), which is in the usual range between the values of 3 (volume-diffusion mechanisms) and 4 (grain-boundary mechanisms) expected for intermediate-stage sintering.<sup>20,21</sup> For grain growth, the slope has a value of  $+0.246$  (regression coefficient of 0.99893).

If we write

$$G \sim t^{1/n}$$

we find  $1/n = 0.246$ , hence  $n \approx 4$ .

If grain growth is grain-boundary controlled, this value of “ $n$ ” suggests a mechanism of diffusion through continuous, Cu-rich, second phase.<sup>22</sup>

#### 4. Conclusions

Additive-free tin-oxide ceramics do not densify, even after sintering at high temperatures (1400°C). However, DTA–TG experiments do not support a common assumption that this behaviour is caused by vaporisation or decomposition of SnO<sub>2</sub>.

Copper oxide is a very effective sintering aid. When using a precursor-plus-powder route, which insures a good dispersion of additive, the optimum content of CuO is close to 0.75 wt.%. This allows high densification ( $\approx 98\%$  of theoretical density) with moderate grain growth.

The sintering process mainly develops in solid state, as shown by the fact that shrinkage begins at temperatures inferior to 800°C, that is well below the melting temperature of the eutectic between CuO and Cu<sub>2</sub>O ( $\approx 1090^\circ\text{C}$ ). There is no evidence of a liquid at low temperature ( $\approx 940^\circ\text{C}$ ), as suggested by Bonnet et al.<sup>13,23</sup> On-heating DTA–TG experiments show that CuO reduces to Cu<sub>2</sub>O (at  $\approx 1050^\circ\text{C}$ ), then Cu<sub>2</sub>O partially re-oxidises to CuO (at  $\approx 1130^\circ\text{C}$ ). On cooling, there is an hysteresis and Cu<sub>2</sub>O residues still exist at room temperature.

Microstructure observations show that the grain boundaries in CuO-containing SnO<sub>2</sub> ceramics are enriched with copper, which suggests that the role of CuO as sintering aid mainly involves grain-boundary mechanisms.

## Acknowledgements

The authors gratefully acknowledge Séverine Le Gac for her helpful assistance.

## References

- Duvigneaud, P. H. and Reighard, D., Activated sintering of tin oxide. In *Science of Sintering*, Vol. 12, ed. P. Vincenzini. Ceramurgia Srl, Faenza, Italy, 1980, pp. 287–292.
- Cerri, J. A., Leite, E. R., Gouvêa, D. and Longo, E., Effect of cobalt(II) oxide and manganese(IV) oxide on sintering of tin(IV) oxide. *J. Am. Ceram. Soc.*, 1996, **79**(3), 799–804.
- Kimura, K., Inada, S. and Yamaguchi, T., Microstructure development in SnO<sub>2</sub> with and without additives. *J. Mater. Sci.*, 1989, **24**(1), 220–226.
- Ahn, J.-P., Park, J.-K. and Huh, M.-Y., Effect of green density on the subsequent densification and grain growth of ultrafine SnO<sub>2</sub> powder during isochronal sintering. *J. Am. Ceram. Soc.*, 1997, **80**(8), 2165–2167.
- Yoshinaka, M., Hirota, K., Ito, M., Takano, H. and Yamaguchi, O., Hot isostatic pressing of reactive SnO<sub>2</sub> powder. *J. Am. Ceram. Soc.*, 1999, **82**(1), 216–218.
- Matsushita, T. and Yamai, I., Effects of oxide additives on sintering of Sb<sub>2</sub>O<sub>3</sub>-doped SnO<sub>2</sub> ceramics. *Yogyo-Kyokai-Shi*, 1972, **80**(8), 305–312.
- Takahashi, J., Kodaira, K., Matsushita, T., Yamai, I. and Saito, H., Effect of V<sub>2</sub>O<sub>5</sub> additive on the sintering of SnO<sub>2</sub>. *Yogyo-Kyokai-Shi*, 1975, **83**(1), 33–37.
- Takahashi, J., Yamai, I. and Saito, H., Effect of Nb<sub>2</sub>O<sub>5</sub> additive on the sintering of SnO<sub>2</sub>. *Yogyo-Kyokai-Shi*, 1975, **83**(7), 362–366.
- Gouvêa, D., Smith, A., Smith, D. S. and Bonnet, J. P., Translucent tin dioxide ceramics obtained by natural sintering. *J. Am. Ceram. Soc.*, 1997, **80**(10), 2735–2736.
- Yuan, D. W., Wang, S. F., Huebner, W. and Simkovich, G., The effect of Li-salt additions on the densification of tin dioxide. *J. Mater. Res.*, 1993, **8**(7), 1675–1679.
- Varela, J. A., Whittemore, O. J. and Longo, E., Pore size evolution during sintering of ceramic oxide. *Ceram. Int.*, 1990, **16**(3), 177–189.
- Dolet, N., Heintz, J. M., Onillon, M. and Bonnet, J. P., Densification of 0.99SnO<sub>2</sub>-0.01CuO mixture: evidence for liquid phase sintering. *J. Eur. Cer. Soc.*, 1992, **9**, 19–25.
- Bonnet, J. P., Dolet, N. and Heintz, J. M., Low-temperature sintering of 0.99 SnO<sub>2</sub>-0.01 CuO: influence of copper surface diffusion. *J. Eur. Cer. Soc.*, 1996, **16**, 1163–1169.
- Henry, M., Bonhomme, C. and Livage, J., Synthesis and characterization of copper (II) hydroxide gels. *Journal of Sol-Gel Science and Technology*, 1996, **6**, 155–167.
- Gadalla, A. M., Ford, W. F. and White, J., *Trans. Br. Ceram. Soc.*, 1963, **62**(1), 57.
- Levin, E., Robbins, C. R. and McMurdie, H. F., *Phase Diagrams for Ceramists* (Supplement) Vol. II. American Ceramic Society Inc, OH, USA (Fig. 2069).
- Shao, Z., Liu, K., Liu, L., Liu, H. and Dou, S., Equilibrium phase diagrams in the systems PbO-Ag and CuO-Ag. *J. Am. Ceram. Soc.*, 1993, **76**(10), 2663–2664.
- Dolet, N., Etudes des Paramètres Régissant le Frittage et les Propriétés Electriques des Céramiques Denses à Base de SnO<sub>2</sub>. Thesis no.742, University of Bordeaux-I, 1992 (in French).
- Scion Image, based on NIH Image for Macintosh by Wayne Rasband, National Institutes of Health, USA, Scion Corporation (<http://www.scioncorp.com>).
- Johnson, D. L., A general model for the intermediate stage of sintering. *J. Am. Ceram. Soc.*, 1970, **53**(10), 574–577.
- Chu, M. Y., Rahaman, M. N., De Jonghe, L. C. and Brook, R. J., Effect of heating rate on sintering and coarsening. *J. Am. Ceram. Soc.*, 1991, **74**(6), 1217–1225.
- Brook, R. J., Controlled grain growth. In *Treatise on Material Science and Technology* — 9, ed. F. Y. Wang. Academic Press, New York, 1976, pp. 331–362.
- Dolet, N., Heintz, J. M., Rabardel, L., Onillon, M. and Bonnet, J. P., Sintering mechanisms of 0.99 SnO<sub>2</sub>-0.01 CuO mixtures. *J. Mater. Sci.*, 1995, **30**, 365–368.